

## Observation of the Rayleigh-Taylor Instability in Ablatively Accelerated Foils

J. Grun, M. H. Emery, S. Kacendar, C. B. Opal, E. A. McLean,  
S. P. Obenschain, B. H. Ripin, and A. Schmitt

*Naval Research Laboratory, Washington, D. C. 20375*

(Received 13 February 1984)

We present the first absolute, two-dimensionally resolved measurements of areal mass density of laser-driven ablatively accelerated foils, which show the Rayleigh-Taylor instability developing from initial mass perturbations. Our data are near simulation results which predict that the Rayleigh-Taylor growth rate is less than classical. The measurements sometimes show development of significant areal mass inhomogeneity in a direction perpendicular to that of the initially imposed perturbations.

PACS numbers: 52.30.+r, 07.85.+n, 47.20.+m, 52.70.-m

The well-known Rayleigh-Taylor (RT) instability develops at the interface of two fluids when a heavier fluid floats on top of a lighter one. Sinusoidal perturbations at the interface grow exponentially, deforming the heavier fluid into protrusions that increase in mass and fall through the lighter fluid, thereby reducing the system's potential energy. The mass which feeds the protrusions is transferred from adjacent regions within the heavier fluid. An analogous RT instability is predicted to occur near the ablation surface of imploding fusion-pellet shells.<sup>1,2</sup> The consequences of this prediction are serious since RT instability, and the resulting variation in shell areal mass density ( $\rho r$ ), could degrade the implosion symmetry and fuel compression to values below those required for high-energy gain. To maintain acceptable implosion symmetry the maximum shell aspect ratio (radius/thickness) would have to be reduced and the laser irradiance increased.

To date, only a few experiments have attempted to verify the fusion-related RT theory.<sup>3-9</sup> Of these, some inferred that RT growth rates are much below theoretical predictions or that ablatively accelerated shells may actually be RT stable.<sup>3,4</sup> More recently, workers at Rutherford Appleton Laboratory<sup>5</sup> and the Naval Research Laboratory,<sup>6,7</sup> using periodically perturbed foils to seed RT instability,<sup>8,9</sup> have measured growths of areal mass nonuniformities,  $\Delta(\rho r)$ , that were closer to numerical simulations.

In this paper, we present the first measurements of absolute  $\rho r$  profiles in RT-unstable foils designed to model ablatively imploding pellet shells. These are also the first RT measurements resolved in the two spatial dimensions perpendicular to the acceleration vector. We have observed two-dimensional effects and the mass transfer predicted

by theory. The experimental  $\rho r$  values are close to those calculated by a hydrodynamic code which predicts RT growth rates that are about  $\frac{1}{2}$  of the classical value of (wave number times acceleration)<sup>1/2</sup>.

The foils in the experiment are ablatively accelerated by a laser to about 100 km/s. The laser pulse (1.054  $\mu\text{m}$ , nearly Gaussian, 5-ns full width at half maximum) is focused to  $10^{13}$  W/cm<sup>2</sup> in a 700- $\mu\text{m}$ -diam spot giving a fairly uniform ( $\pm 30\%$ ) flat-topped irradiance profile on the foil surface. The rear surface of the foil is grooved in a square-wave pattern so as to perturb its initial areal mass density. This promotes the growth of the instability at predetermined wavelengths and makes the instability easier to identify.

In-flight areal mass density is measured with a face-on x-ray backlighting method described in detail elsewhere.<sup>10</sup> Briefly, a thin ( $\sim 0.1 \mu\text{m}$ ) magnesium strip, which serves as a backlighter, is buried beneath a plastic coating on the smooth, laser side of a perturbed carbon foil. The plastic coating is thinner than the ablation depth, allowing the laser to heat the magnesium during acceleration, and thereby producing a pulse of backlighting x rays (1.3 keV). These x rays are viewed by three aluminum-filtered pinhole cameras: one camera on the laser side of the foil photographs the source; a second camera at the rear of the foil records the radiograph; and a third camera on the laser side of the foil, looking through a stepped carbon filter, calibrates the x-ray backlighter and the film on each shot. From the source photograph and the radiograph a spatially two-dimensional, absolute areal mass density profile is reconstructed. X-ray source nonuniformities are totally accounted for in this reduction by matching each point on the radiograph

with the corresponding point on the source.

The timing of the x-ray flash (2-ns full width at half maximum duration) with respect to the laser pulse is measured by use of fast (300 ps), MRD 500 *p-i-n* diodes, one of which has its window replaced by an aluminum filter to make it sensitive to x rays. Values of  $\rho r$ , for our data, averaged over the flash duration are within 3% (13%) of  $\rho r$  at the flash peak for the thick (thin) parts of the foil. This was determined theoretically by comparing the transmission of 2-ns-long and instantaneous x-ray flashes through RT-unstable foils, where RT growth was calculated by our code.

On each shot the rear surface temperatures of the perturbed foils are measured with time-resolved optical pyrometry.<sup>11</sup> This is done to make sure that the foils were ablatively accelerated without catastrophic breakup which would permit front surface plasma ( $\approx 500$  eV) to be seen from the rear. The rear temperatures of the initially perturbed foils were  $\leq 5$  eV and were about the same as the temperatures measured in unperturbed foils.

Perturbation growth and foil acceleration history are calculated with the Eulerian FAST2D code<sup>12</sup> which solves the ideal hydrodynamic equations with classical thermal conduction using flux-corrected transport algorithms. This code has been compared to measurements of hydrodynamic efficiencies, mass ablation rates, ablation pressures, foil velocities, blowoff-plasma velocities, and blowoff-plasma profiles for unperturbed foils, and was found to give accurate results.<sup>13,14</sup> For our experiment, carbon/plastic foils are modeled by all-carbon foils of equivalent areal mass density that have reached steady state at  $\frac{1}{50}$  of the peak irradiance. The magnitudes and wavelengths of the initial areal mass density perturbations are the same as in the experiment. Peak irradiance, however, is not input directly from the experiment because lateral thermal transport and spatial profile shape make an accurate irradiance measurement difficult. Instead, we measure the asymptotic speed of an unperturbed foil with a double-foil method<sup>14</sup> and then adjust the code's peak irradiance (to  $1.4 \times 10^{13}$  W/cm<sup>2</sup>) until the calculated and measured velocities match. This procedure calibrates the code to the experiment. At the laser pulse peak, the code predicts a rear-side foil temperature of 4–7 eV and a maximum density nearly twice that of solid carbon.

We have measured the increase in  $\Delta(\rho r)$  due to the RT instability in foils perturbed with a 30-, 46-, and 100- $\mu$ m period. Figure 1(a) is the x-ray source emission, which peaked at 0.5 ns past the laser maximum, and Fig. 1(b) is the radiograph of a foil

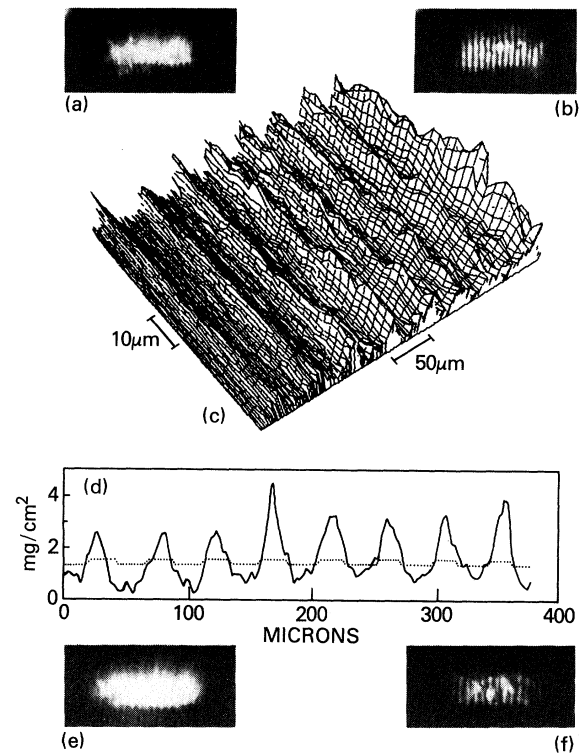


FIG. 1. Sample results: (a) x-ray source photograph (front foil view) and (b) radiograph (rear foil view) of a 1.2-mg/cm<sup>2</sup>-C plus 0.28-mg/cm<sup>2</sup>-plastic foil with a 46- $\mu$ m period,  $\Delta(\rho r)/\langle\rho r\rangle=0.14$  initial perturbation, accelerated to 80 km/s. (c) Areal mass density profile deduced from (a) and (b). (d) A cut across the areal mass density profile (solid line) compared to the initial foil perturbation (dashed line). (e) X-ray source photograph and (f) radiograph of a 1.0-mg/cm<sup>2</sup>-C plus 0.22-mg/cm<sup>2</sup>-plastic foil with a 46- $\mu$ m period,  $\Delta(\rho r)/\langle\rho r\rangle=0.13$  initial perturbation, accelerated to 100 km/s. The backlighter x rays in (a) peaked at 0.5 nsec past the maximum of the laser pulse. The data in (e) and (f) were taken at about the same time as (a) and (b). In (b) and (f) bright regions occur where the foil is thin. In (a) and (b) the laser pulse was longitudinally multimoded and we assumed that this had a negligible effect. In (e) and (f) the laser was not multimoded.

with a 46- $\mu$ m-period initial perturbation. Note that the x-ray emission is modulated at the perturbation wavelength. The areal mass density profile (accurate to within 30%)<sup>15</sup> is shown in Fig. 1(c), and a cut across the profile in Fig. 1(d). Spikes with  $\rho r$  about twice that of the original foil have developed, which clearly shows the occurrence of mass transfer from the thin to the thick parts of the foil, as is expected from RT theory. In addition, the measured [Fig. 1(d)] and simulated [Fig. 2(a)]  $\rho r$  profiles agree well.

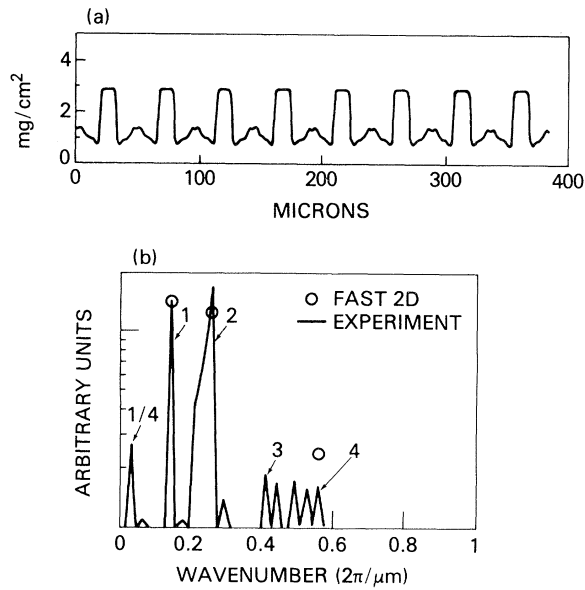


FIG. 2. Simulation of foil in Figs. 1(a)–1(d): (a) Areal mass density profile obtained from the FAST2D code. (b) Comparison of simulated and experimental mode spectra. The experimental mode spectrum is obtained from Fig. 1(c) after averaging along the thick and thin foil sections. Spectra are normalized at the fundamental and the dc mode is not shown.

The dominant modes in both the measurement and the simulation are the fundamental and the second harmonic. Strong growth of the second harmonic is surprising since it is not a mode of a square-wave perturbation. However, FAST2D shows that the second harmonic is seeded—early in time—by vortices that appear at the rear surface of the foil (where the initial perturbations are) as it begins to accelerate. These vortices, which develop as a result of strong noncollinear pressure and density gradients,<sup>16</sup> feed low-density material from the initially thicker parts of the foil to the initially thinner parts increasing the areal mass density in the center of the thin part. This perturbs the second harmonic which then undergoes RT growth. Second-harmonic growth in the experiment may also conceivably arise from imperfections in the foil or laser beam spatial profile—mechanisms that we cannot absolutely rule out. Nevertheless, as Fig. 2(b) shows, the measured and simulated amplitudes of the second harmonic agree well.

Besides the two dominant modes other much weaker modes at one-quarter harmonic and between the third and fourth harmonics are seen experimentally. These modes may be real or may be induced by the choice of box size in the fast-Fourier-transform algorithm. The code predicts the

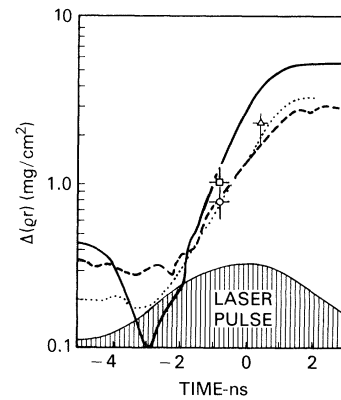


FIG. 3. Measured and simulated  $\Delta(\rho r)$  for three cases: Circle and solid line, 1.6-mg/cm<sup>2</sup>-C plus 0.22-mg/cm<sup>2</sup>-plastic foil with a 30- $\mu$ m period,  $\Delta(\rho r)/\langle\rho r\rangle = 0.23$  initial perturbation, accelerated to 60 km/s. The laser pulse, on this shot, was longitudinally multimoded and we assumed that this had a negligible effect. Square and dashed line, 1.2-mg/cm<sup>2</sup>-C plus 0.22-mg/cm<sup>2</sup>-plastic foil with a 100- $\mu$ m period,  $\Delta(\rho r)/\langle\rho r\rangle = 0.24$  initial perturbation, accelerated to 80 km/s. Triangle and dotted line, case described in Fig. 1. Systematic errors are estimated by the bars.

existence of weak third and fourth harmonics. Both, however, oscillate while growing making a comparison to experiment difficult.

Rayleigh-Taylor growth and the calculated evolution of the instability for this and the two other wavelengths are shown in Fig. 3. The code predicts that after a delay during which no perturbation growth occurs a RT eigenmode is excited and the instability increases exponentially at rates of  $9.8 \times 10^8$ ,  $7.6 \times 10^8$ , and  $5.8 \times 10^8$  s<sup>-1</sup> versus  $18 \times 10^8$ ,  $12 \times 10^8$ , and  $9.8 \times 10^8$  s<sup>-1</sup> classical for the 30-, 46-, and 100- $\mu$ m case, respectively. (A similar reduction in RT growth rate is calculated for foils with very small,  $\sim 1\%$ , initial perturbations.) Then the laser runs out of power and/or the growth is saturated. Figure 3 compares the predicted and measured  $\Delta(\rho r)$ . The agreement between the measurement and code is again reasonable. Note, however, that a definite experimental test of RT growth rates awaits measurement of the evolution of the instability.

On some shots we observed bubble expansion and the coalescing of adjacent bubbles. For example, consider the radiograph in Fig. 1(f). Here, an expansion of a bubble into an egg shape can be seen near the center of the photograph; to the right of it two bubbles are merging and to the left a thin region is expanding locally in two places. Analysis of the areal mass density (accurate to 10% on this

shot)<sup>15</sup> indicates that these nonuniform regions are so thin that the target is about to break up in these places. These nonuniformities are qualitatively similar to the two-dimensional material flow patterns that have been predicted for a foil RT unstable in a plane.<sup>2</sup> Growth in a direction perpendicular to the initial foil perturbations could have been stimulated by laser-beam-profile nonuniformities.

In conclusion, we have measured absolute, two-dimensionally resolved  $\rho r$  profiles in initially perturbed, RT-unstable foils. We have observed the mass-transfer signature of RT instability and interesting features qualitatively similar to those predicted by three-dimensional RT theory. The increase in  $\Delta(\rho r)$  due to RT instability is close to that predicted by simulations. Determination of accurate rates, however, awaits measurements of the evolution of the instability.

The authors thank S. Bodner and R. Whitlock for stimulating discussions, and E. Turbyfill, N. Nocerino, and B. Sands for their technical assistance. The excellent work of J. Kosakowski and M. Fink who constructed the perturbed targets described here is very much appreciated. This work was supported by the U.S. Department of Energy and the Defense Nuclear Agency.

---

<sup>1</sup>Some theory: J. N. Shiau *et al.*, Phys. Rev. Lett. **32**, 352 (1974); J. D. Lindl and W. C. Mead, Phys. Rev. Lett. **34**, 1273 (1975); R. L. McCrory *et al.*, Phys. Rev. Lett.

**46**, 336 (1981); M. H. Emery *et al.*, Phys. Rev. Lett. **48**, 677 (1982); K. O. Mikaelian, Phys. Rev. Lett. **48**, 1365 (1982); R. G. Evans *et al.*, Phys. Rev. Lett. **49**, 1639 (1982).

<sup>2</sup>D. Colombant *et al.*, to be published.

<sup>3</sup>A. Raven *et al.*, Phys. Rev. Lett. **47**, 1049 (1981).

<sup>4</sup>J. D. Kilkenny *et al.*, J. Phys. D **13**, L123 (1980).

<sup>5</sup>A. J. Cole *et al.*, Nature (London) **299**, 329 (1982).

<sup>6</sup>J. Grun *et al.*, in Abstracts of the Thirteenth Annual Anomalous Absorption Conference, Alberta, Canada, 5–10 June 1983 (unpublished), and in Proceedings of the European Conference on Laser Interaction with Matter, London, 26–30 September 1983 (unpublished).

<sup>7</sup>R. R. Whitlock *et al.*, Phys. Rev. Lett. **52**, 819 (1984).

<sup>8</sup>B. H. Ripin *et al.*, Bull. Am. Phys. Soc. **25**, 946 (1980); J. Grun *et al.*, Bull. Am. Phys. Soc. **26**, 1023 (1981).

<sup>9</sup>J. Grun *et al.*, Naval Research Laboratory Memorandum Report No. 4896, 1983 (unpublished).

<sup>10</sup>J. Grun and S. Kacenjar, Appl. Phys. Lett. **44**, 497 (1984).

<sup>11</sup>E. A. McLean *et al.*, Phys. Rev. Lett. **45**, 1246 (1980).

<sup>12</sup>J. P. Boris, Comment Plasma Phys. Controlled Fusion **3**, 1 (1977); M. H. Emery *et al.*, Phys. Rev. Lett. **48**, 253 (1982).

<sup>13</sup>NRL Plasma Interaction Group, Naval Research Laboratory Memorandum Report No. 4369, 1980 (unpublished); J. Grun *et al.*, Appl. Phys. Lett. **39**, 545 (1981); P. G. Burkhalter *et al.*, Phys. Fluids **26**, 3650 (1983).

<sup>14</sup>J. Grun *et al.*, Phys. Fluids **26**, 588 (1982).

<sup>15</sup>The actual target mass beneath the backlighter and the mass calculated from the areal mass density profile are the same to within the accuracy stated in the text.

<sup>16</sup>M. H. Emery *et al.*, Naval Research Laboratory Memorandum Report No. 5089, 1983 (to be published).

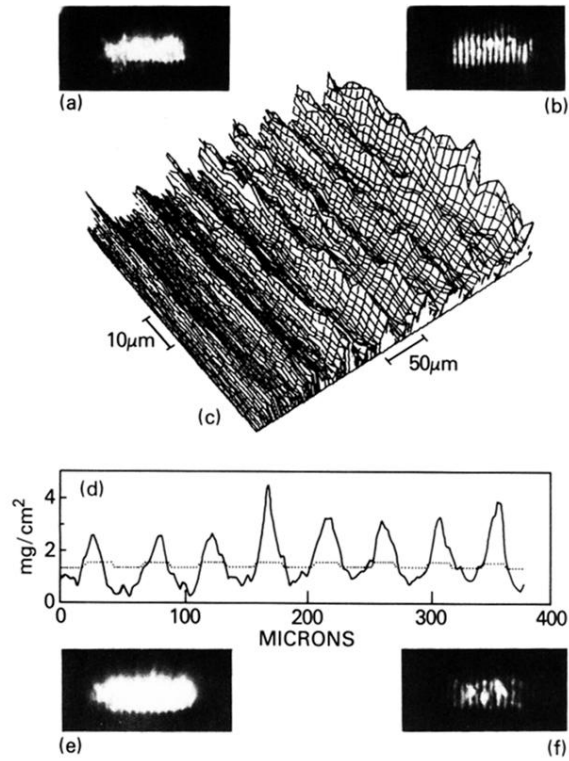


FIG. 1. Sample results: (a) x-ray source photograph (front foil view) and (b) radiograph (rear foil view) of a  $1.2\text{-mg/cm}^2\text{-C}$  plus  $0.28\text{-mg/cm}^2\text{-plastic}$  foil with a  $46\text{-}\mu\text{m}$  period,  $\Delta(\rho r)/\langle\rho r\rangle = 0.14$  initial perturbation, accelerated to  $80\text{ km/s}$ . (c) Areal mass density profile deduced from (a) and (b). (d) A cut across the areal mass density profile (solid line) compared to the initial foil perturbation (dashed line). (e) X-ray source photograph and (f) radiograph of a  $1.0\text{-mg/cm}^2\text{-C}$  plus  $0.22\text{-mg/cm}^2\text{-plastic}$  foil with a  $46\text{-}\mu\text{m}$  period,  $\Delta(\rho r)/\langle\rho r\rangle = 0.13$  initial perturbation, accelerated to  $100\text{ km/s}$ . The backlighter x rays in (a) peaked at  $0.5\text{ nsec}$  past the maximum of the laser pulse. The data in (e) and (f) were taken at about the same time as (a) and (b). In (b) and (f) bright regions occur where the foil is thin. In (a) and (b) the laser pulse was longitudinally multimoded and we assumed that this had a negligible effect. In (e) and (f) the laser was not multimoded.